Proceedings of the 14th IASTED International Conference
Robotics and Applications (RA 2009)
November 2 - 4, 2009 Cambridge, MA, USA

DESIGN OF SELF-ADJUSTING ORTHOSES FOR REHABILITATION

Dung Cai, Philippe Bidaud, Vincent Hayward
Institut des Système Intelligents et de Robotique (ISIR)
Université Pierre et Marie Curie
Pyramide - T55/65 CC 173 - 4 Place Jussieu
75005 Paris, France
cai,bidaud,hayward@isir.upmc.fr

Florian Gosselin
CEA LIST, Sensory Interfaces Laboratory
18 route du Panorama, BP6, F-92265
Fontenay Aux Roses, France
florian.gosselin@cea.fr

ABSTRACT
Safety and comfort are primary concerns in rehabilitation devices and exoskeletons. However, the result of using simplified kinematic arrangements can be discomfort, or even injury, as a result of overconstraining the joint. In this paper, we describe a self-adjusting mechanism able to overcome misalignment between the rotational axis of the mechanism that is attached to the user's limbs and the rotational axis of the anatomical joint. Additional degrees of freedom are added to the mechanism to eliminate internal residual forces. Furthermore, a new technique for the estimation of the Instantaneous Center of Rotation of the assisted joint based on velocity and position sensors is demonstrated. We illustrate this technique with a mechanism which is able to self-adjust with or without resorting to motorized add-ons. Kinematic analyses are presented and are validated by computer simulation on 2D examples.

KEY WORDS
Self-adjusting mechanism, Estimation of ICR

1 Introduction

An orthosis is a mechanical support designed to compensate or to correct a deficient function in a joint. It can be used, for example, to improve the physiological efficiency of a limb that has lost its function due to trauma or disease, or that has been affected by a congenital anomaly. Many types of passive orthoses have been developed over the years, especially for lower limb rehabilitation. Lower limb guidance orthoses are devices attached externally to a lower body segment in order to control its motion, to provide mechanical stabilization, to reduce discomfort by transferring load to another area, to correct anomalies, and to prevent the progression of deformities. One of the functions that is specific to knee orthoses is the control of the anterior translation of the tibia, as well as its rotation during knee flexion (bending) and knee extension (straightening). As illustrated in Fig. 1, a typical articulated knee orthosis has inner and outer guide plates that are connected to the joints by adjustable

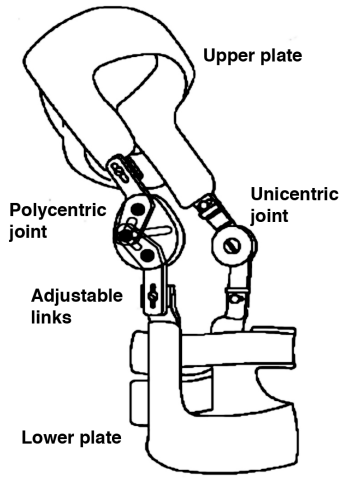

Figure 1. Example of knee orthosis with one polycentric joint - Image adapted from Herzberg and al. [1]

links. The plates are shaped to fit the anatomy of the thigh and of the leg. The plates are linked together by unicentric or polycentric hinges mounted on sliding elements to be adjusted to locate the joint axis to an optimum. Prefabricated orthoses with unicentric hinges can be used in simple applications such as to enhance lateral stabilization. A polycentric pivot joint is better able to track the anatomical knee throughout its range of motion [2] [3] [4] [5] [6]. It allows natural knee flexure and high lateral support thus ensuring good control of the limb motion. These more complex designs are used in orthoses that are developed in the case of complex pathologies or for postoperative treatments. Because of the inter-individual variability in joint kinematics [7] [8] [9], these orthoses must be made-to-measure.

Muscular strengthening devices and power suit devices must also provide a motion that tracks human joint kinematics in order to avoid damage to the joints. A typical approach is to allow some freedom between the natural and the artificial kinematics, for instance by connecting the natural and the artificial limbs at the end-point [10], [11]. End-point-

based designs, however, are known to force natural joints in arbitrary directions, possibly causing hyperextension [12]. For devices that are attached to the limbs, the axis of rotation must be in coincidence with the rotation axis of the anatomical joint as much as possible [13], just as in the case of a passive orthosis. Then, the question of approximating the natural kinematics with an artificial system arises similarly, since misalignments between the two systems generate undesirable residual forces and torques to the limb. The consequences of an inadequate design can range from reduced comfort to permanent injury.

A device that can be safe and comfortable must be able to reproduce the natural human joint kinematics accurately. Such design must have two functions: It must be able to estimate the kinematics of a natural joint which has an inter-individual variability and which can change in time, and then self-adjust its geometry to match the kinematics of the natural joint as closely as possible.

In the next section, a 2D kinematic model of the system is presented to demonstrate how the proposed mechanical solution makes it possible to estimate the instantaneous center of rotation of a joint. In section 3, the self-adjustment property of the mechanism in the direction of the axis of the thigh is analyzed. This property facilitates the implementation of the mechanism on the users' limbs and has been leveraged by designers of knee orthosis devices. Finally, simulation models are used to demonstrate and validate these properties in section 4.

2 Kinematic model

2.1 System modeling

Fig. 2 shows a simple model of the proposed system. A slider-pin and a slider-joint are placed and attached to the limbs in their anterior plan. This configuration is selected in order to obtain a better stability. It will also ease a three-dimensional design for more complex cases. Segments PM and PB represent the limbs. A pin joint is placed at location B in order to account for the flexibility of the attachment deformable tissues. We assume, however, that the mechanism is rigidly attached to the first limb. Since the attachment location is arbitrary, point M is defined such that the segment MN is orthogonal to segments PM and AN. Point K is on the segment BH such that segments PK and BH are orthogonal.

Let γ_0 be the initial value of the angle $\widehat{PBH} = \theta_4$ when the device is first attached. Misalignment can be modeled as the energy stored in a torsional spring centered in B with stiffness k. The torsional torque, C_B, caused by misalignment is

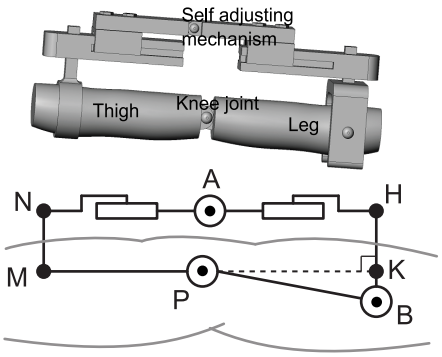

Figure 2. The first model of the problem. A pin joint P is used to represent the user's joint. B is the attachment point. M is chosen such that the segment PM which represents the higher limb and the segment AN of the mechanism are parallel, and the segments MN and PM are orthogonal.

$$C_B = k(\widehat{PBH} - \gamma_0). \quad (1)$$

As further shown below, self-adjustment is achieved by this arrangement, since during movements, the system will tend to minimize the elastic energy stored in the torsional spring. The torque produced by this spring will generate the self-adaption movement. For the design of a prototype, a pin joint and a torsional spring can be inserted at point B. The pin joint will reduce the residual torque on tissues layers and the spring will provide the auto-adjustment property. It is also possible to rely on the flexibility of the tissue of and the skin to act as a flexible energy storage. The second choice is simpler but the residual torque could reduce the comfort of the user. From now on we will consider point B to be a pin joint with a torsional spring.

The complete model of the system is shown in the Fig. 3 where $\dot{r_1}$ is the linear velocity of the part (1) relative to (0), $\dot{\theta_2}$ is the angular velocity of the part (2) relative to (1), $\dot{r_3}$ is the linear velocity of the part (3) relative to (2), $\dot{\theta_4}$ is the angular velocity of the part (4) relative to (3), and $\dot{\theta_5}$ is the angular velocity of the part (0) relative to (4).

The velocity of the user's rotational joint can be expressed at point P as:

$$V(P) = \begin{pmatrix} \dot{x_P} \\ \dot{y_P} \\ \dot{q_P} \end{pmatrix} = J_P(q) \begin{pmatrix} \dot{r_1} \\ \dot{\theta_2} \\ \dot{r_3} \\ \dot{\theta_4} \\ \dot{\theta_5} \end{pmatrix}. \quad (2)$$

$\dot{x_P}$ and $\dot{y_P}$ are the components of the linear velocity of the point P relative to (0). $\dot{q_P}$ is the angular

velocity of the point P relative to (0). As P is a rotational joint, $\dot{x_P}$ and $\dot{y_P}$ are equal to zero.

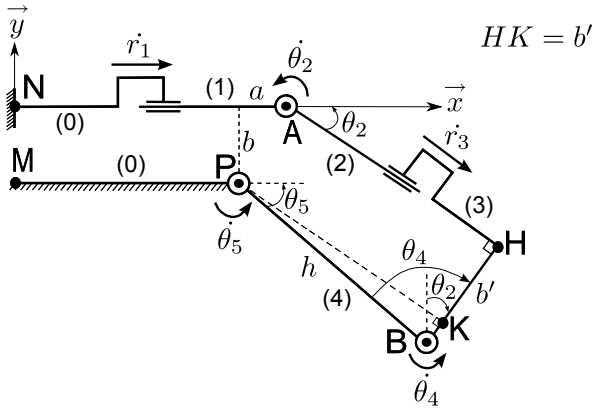

Figure 3. Model of the mechanism structure

The Jacobian matrix of the whole system can be written in the coordinate frame $R_1 = (A, \vec{x}, \vec{y})$ at the point P as:

$$J_P(q) = \begin{pmatrix} 1 & b & \cos\theta_2 & -h\cos(\theta_4 - \theta_2) & 0 \\ 0 & -a & -\sin\theta_2 & -h\sin(\theta_4 - \theta_2) & 0 \\ 0 & 1 & 0 & 1 & 1 \end{pmatrix}. \tag{3}$$

(a,b) are components of the vector $\vec{PA}$ in the coordinate frame $R_1 = (A, \vec{x}, \vec{y})$.

2.2 Estimation of the instantaneous center of rotation of the human joint

Given the Jacobian matrix (3), we apply the loop closure constraint at P which provides the following system of equation,

$$\begin{cases} \dot{r_1} + b\dot{\theta_2} + \dot{r_3}\cos\theta_2 - \dot{\theta_4}h\cos(\theta_4 - \theta_2) = 0, \\ -a\dot{\theta_2} - \dot{r_3}\sin\theta_2 - \dot{\theta_4}h\sin(\theta_4 - \theta_2) = 0, \\ \dot{\theta_2} + \dot{\theta_4} = -\dot{\theta_5}. \end{cases} \tag{4}$$

If we secure the attachment at the point B so that the angle θ_4 will remain constant during the movement (the other joints are supposed to be ideal and the effects of friction are neglected), then the whole system can be considered to have only one degree of freedom. Therefore $\dot{\theta_4} = 0$, and we can write a and b as:

$$a = -\frac{\dot{r_3}\sin\theta_2}{\dot{\theta_2}}. \tag{5}$$

$$b = -\frac{\dot{r_3}\cos\theta_2 + \dot{r_1}}{\dot{\theta_2}}. \tag{6}$$

The location of the Instantaneous Center of Rotation (ICR) can be estimated by using the two expressions above, which require the measurement of the angular rotation of the pin joint and the velocities of the mechanism's joints.

3 Self-adjustment property

3.1 Mechanical constraint during the attachment phase

It can be easily demonstrated that if during the movement of the limbs, the location of P and the value of the angle θ_4 remain unchanged, then the distance b' between P and the segment AH ($b' = HK$) will be also constant. So if $b \neq b'$ (where $b = MN$ is the distance between P and the segment AN, which is also constant), the mechanism can not reach the position where the segments AN and AH are collinear without any deformation at the attachment joint B. In order to avoid this phenomenon, the two distances b and b' must be equal, which means that the mechanism must be placed at its singular position during the attachment to the limbs.

3.2 Analysis of the singularity model

When the mechanism is in its singular position, its particular geometry will lock the movement of flexion-extension of the limbs. As there is a flexibility in the joint B, a deformation will take place in B that will modify the value of the angle θ_4 and will then allow the mechanism to move away from its singular position. Then, the energy stored in B will act as a rotative actuator and will produce a movement of self-adjustment for the mechanism. The mechanism will then move to the ideal position where $\theta_4 = \gamma_0$. We will demonstrate that, if the location of the point P remains constant during the flexion motion, the segment formed by the two centers of rotation will be located in the symmetry plan of the mechanism.

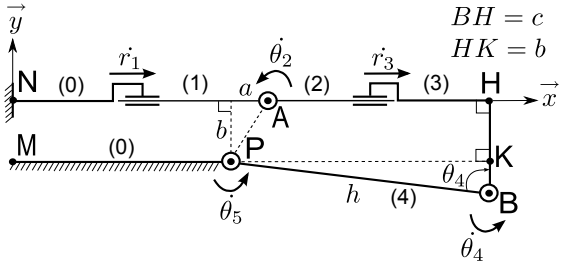

Figure 4. The mechanism in its singular configuration

When the mechanism is in its singular configuration (Fig. 4), $\theta_2 = 0$, $HK = b$ and $BK = c - b = PB\cos\gamma_0$. The system of equations becomes:

$$\begin{cases} \dot{r_1} + b\dot{\theta_2} + \dot{r_3} - \dot{\theta_4} h\cos(\gamma_0) = 0, \\ -a\dot{\theta_2} - \dot{\theta_4} h\sin(\gamma_0) = 0, \\ \dot{\theta_2} + \dot{\theta_4} = -\dot{\theta_5}. \end{cases} \quad (7)$$

The angle $\dot{\theta_4}$ can now be calculated according to $\dot{\theta_2}$ when $\pi > \gamma_0 > 0$,

$$\dot{\theta_4} = -\frac{a\dot{\theta_2}}{h\sin(\gamma_0)}. \quad (8)$$

When $a = 0$, $\dot{\theta_4} = 0$. If the user moves her or his limb, the angular velocity of the pin joint B will be equal to zero. The mechanism escapes from its singular position without any modification of the value of the angle θ_4. Afterward, the angle θ_4 will remain constant during the whole movement.

If $a \neq 0$ and if $\dot{\theta_4} = 0$, which means that the value of the angle θ_4 is constant, we shall obtain $\dot{\theta_2} = 0$ and $\dot{\theta_2} = \dot{\theta_5} \neq 0$ by (7) which leads to a contradiction. There is no possible movement, therefore $\dot{\theta_4}$ is inevitably different from zero. As a result, the torsional spring placed at B will move away from its equilibrium position. The source of energy stored by this spring will then act as an actuator to generate the self-adaption movement of the mechanism.

3.3 Analysis of the self-adaption movement

The Fig. 5 shows a model for the study of the self-adaption motion. For the analysis of this property, the limbs of the user are supposed to be fixed ($\dot{\theta_5} = 0$) during the self-adaption motion.

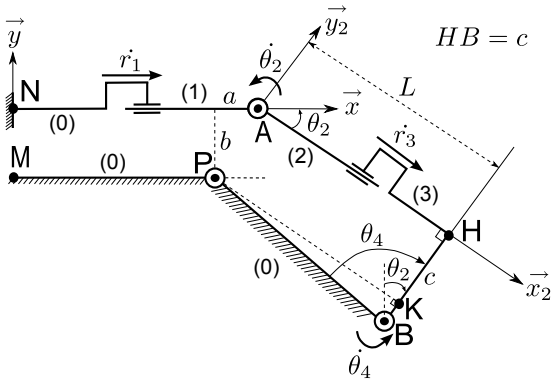

Figure 5. The mechanism's model in a brief interval of time when the user's limbs are considered as fixed

The Jacobian matrix written in the coordinate frame $R_2 = (A, \vec{x_2}, \vec{y_2})$ at the point B is:

$$J_B(q) = \begin{pmatrix} \cos\theta_2 & c & 1 & 0 \\ \sin\theta_2 & L & 0 & 0 \\ 0 & 1 & 0 & 1 \end{pmatrix}. \quad (9)$$

$(-L,c)$ are components of the vector $\vec{BA}$ in the coordinate frame $R_2 = (A, \vec{x_2}, \vec{y_2})$.

The loop closure at B provides the following system of equations:

$$\begin{cases} \dot{r_1}\cos\theta_2 + c\dot{\theta_2} + \dot{r_3} = 0, \\ \dot{r_1}\sin\theta_2 + L\dot{\theta_2} = 0, \\ \dot{\theta_2} = -\dot{\theta_4}. \end{cases} \quad (10)$$

When $\theta_2 = 0$, if $L \neq 0$ then $\dot{\theta_2} = \dot{\theta_4} = 0$, $\dot{r_1} = -\dot{r_3}$ and $\theta_4 = \gamma_0$ respectively. There is no possible angular movement but there is an internal mobility which allows the two prismatic joints to slide and move away from their rest position if there is an external load (for example: the gravity force). We notice that this result can also be obtained by the precedent analysis of the singularity model.

When $\theta_2 \neq 0$, we obtain:

$$\dot{\theta_2} = -\dot{\theta_4},$$

$$\dot{r_1} = -\frac{L\dot{\theta_2}}{\sin\theta_2},$$

$$\dot{r_3} = \frac{(L\cos\theta_2 - c\sin\theta_2)}{\sin\theta_2}\dot{\theta_2}.$$

When $L\cos\theta_2 > c\sin\theta_2$ or $\tan\theta_2 < \frac{L}{c}$, $\dot{r_1}$ and $\dot{r_3}$ will have opposite signs which means that they will slide in the same direction. The mechanism will move to its equilibrium position where $\dot{\theta_4} = 0$ (or $\theta_4 = \gamma_0$). We also notice that the value of c depends on the position of the point A. The nearer the distance between the points A and P is, the smaller the value of c will be, thus it will be easier to obtain the self-adaption motion.

3.4 Kinematic analysis of the mechanism during its motion after the self-adaption

Now let us consider the case where the mechanism is already readjusted, $\theta_4 = \gamma_0$. And in its posterior movement, this angle θ_4 can be considered to be unchanged (because of the resistance of the torsional spring at B). Thus we obtain $HK = PH_2 = b$ and $BK = c - b$ whatever the value of the angle θ_2 is. In this particular case, the joint B can be considered to be a clamp to the limb so it can be neglected in the model. The instantaneous center of rotation of the limbs P is considered to be fixed. The whole system 'mechanism-limbs' can be remodeled as shown in the Fig. 6.

The Jacobian matrix written at the point P, in the frame $R_2 = (A, \vec{x_2}, \vec{y_2})$ is:

$$J_P(q) = \begin{pmatrix} \cos\theta_2 & l\cos\theta & 1 & 0 \\ \sin\theta_2 & l\sin\theta & 0 & 0 \\ 0 & 1 & 0 & 1 \end{pmatrix} \quad (11)$$

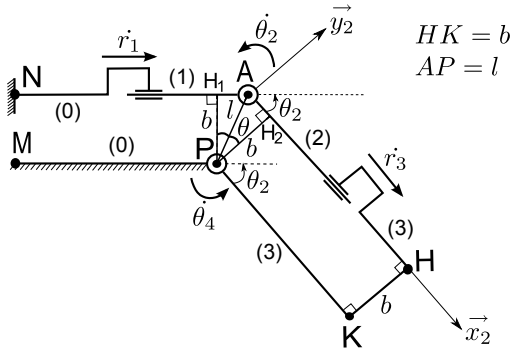

Figure 6. The model when θ_4 is unchanging during motion

$HK = b$, thus $PH_1 = PH_2 = b$. The value of the angles $(\widehat{APH_1})$ and $(\widehat{APH_2})$ are:

$$(\widehat{APH_1}) = (\widehat{APH_2}) = arccos(\frac{b}{l}) = \theta, \qquad (12)$$

with $PA = l$. The value of the angle θ_2 is thus :

$$\theta_2 = (\widehat{APH_1}) + (\widehat{APH_2}) = 2\theta. \qquad (13)$$

The expression (12) shows that the segment AP is located at the symmetry axis (or symmetry plan in 3D) of the mechanism. The loop closure at P provides the following system of equations:

$$\begin{cases} \dot{r_1}\cos\theta_2 + \dot{\theta_2} l\cos\theta + \dot{r_3} = 0, \\ \dot{r_1}\sin\theta_2 + \dot{\theta_2} l\sin\theta = 0, \\ \dot{\theta_2} = -\dot{\theta_4}, \end{cases} \qquad (14)$$

$$\dot{r_1} = -\frac{\dot{\theta_2} l\sin\theta}{\sin\theta_2}, \qquad (15)$$

$$\dot{r_3} = \frac{\dot{\theta_2} l\sin(\theta - \theta_2)}{\sin\theta_2}. \qquad (16)$$

Since $\theta_2 = 2\theta$, according to (13), we obtain :

$$\dot{r_3} = -\frac{\dot{\theta_2} l\sin\theta}{\sin\theta_2}. \qquad (17)$$

Thus,

$$\dot{r_3} = \dot{r_1}. \qquad (18)$$

In this particular case, the point P remains at the symmetry axis of the mechanism. The two prismatic joints slide in the opposite directions with equal speeds. We point out that when l tend towards zero, the velocities $\dot{r_3}$ and $\dot{r_1}$ will also tend towards zero, which means that the slider's motions are insignificant when the rotation axis of the mechanism is close to the rotation axis of the limbs.

The conclusion of this study is that the Slider-Pin-Slider mechanism realizes auto-adjustment of the pin joint regarding to the limbs. The mechanism must be attached to the limbs in its singular position. When the mechanism escapes from its singular position, the restoring torque at the attachment will act as a passive actuator and will move the mechanism to its new position where the center of rotation of the limbs will be located in the symmetry plan of the mechanism. Then the two prismatic joints slide in opposite directions at the same speed (if the ICR of the limbs remains unchanged during motion). When the ICR moves, the two slider joints will slide with different velocities. If we measure their velocities and also the angular velocity of the pin joint, it will be possible to track this variation of the ICR of the human joint.

4 Simulation

4.1 Simulation of the self-adaption property

A dynamic simulation (Cosmosmotion, SolidWorks) is used to verify the results. Two simulations were carried out for two different mechanisms: The slider-pin-slider mechanism and the slider-multipleparallelogram-slider mechanism. The second mechanism is similar to the first one. The difference is that its virtual axis of rotation is closer to the center of rotation of the limbs [14].

In this simulation, the limbs are set to rotate at a constant angular velocity (5 degree/s). A torsional spring (1 N.m/degree) is added to the pin joint of the attachment of the second limb. The friction coefficient of the two sliders is set at 0.005.

The Fig. 8 and 9 show different images of the mechanisms during simulation. In the 1st image, we can see that the rotation axes aren't in their appropriate positions. The 2nd image shows the adjustment motion. The mechanism moves the pin joint axis (or multiple-parallelograms unit) to the new position where the rotation axis of the limbs would be located in the symmetry plans of the mechanisms.

The figures 10, 11, 12 and 13 show the simulation's results of the slider-pin-slider mechanism and the slider-multipleparallelogram-slider mechanism. We can point out that the auto-adjustment movements takes place respectively at 1.48 second and 1.50 second in each case, the two sliders realize wide displacements in order to lead the mechanism to the equilibrium position. Afterward, they slide slowly at the same linear speed. The angular velocity of the pin joint fluctuates during the auto-adjustment motion and becomes equal to the angular velocity of the user's limbs again once the mechanism is readjusted. The simulation shows that the self-adaption movement takes place sooner with the slider-multipleparallelogram-slider mechanism because its instantaneous axis of rotation is closer to the human joint. This result verifies the

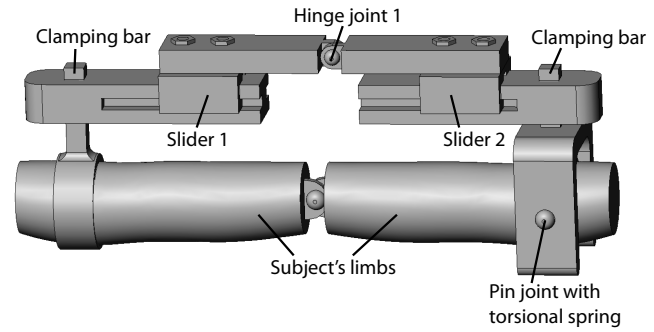

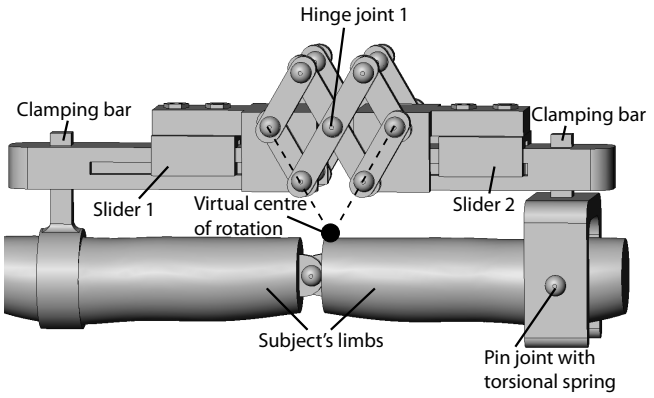

Figure 7. The mechanisms used in simulation. (a) The mechanism slider-pin-slider. (b) The mechanism slider-multipleparallelogram-slider

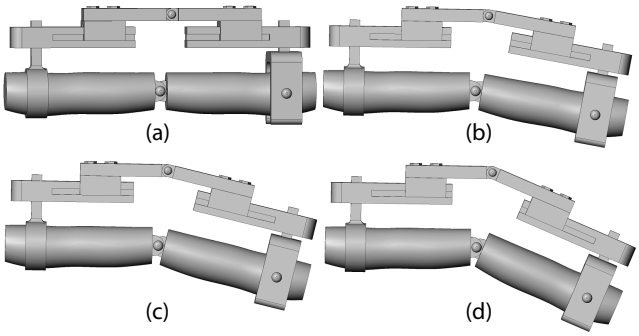

Figure 8. The configuration of the mechanism slider-pin-slider during simulation. (a) The mechanism at its initial position. (b) The mechanism before the self-adaption movement. (c) The mechanism at the self-adaption movement. (d) The mechanism after the self-adaption movement

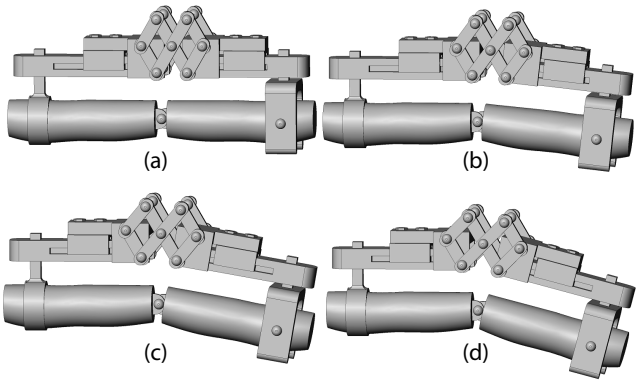

Figure 9. The configuration of the mechanism slider-multipleparallelogram-slider during simulation. (a) The mechanism at its initial position. (b) The mechanism before the self-adaption movement. (c) The mechanism at the self-adaption movement. (d) The mechanism after the self-adaption movement

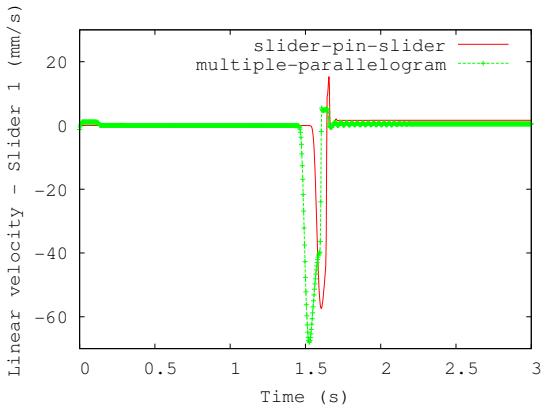

Figure 10. Simulation's result: linear velocity of the slider 1

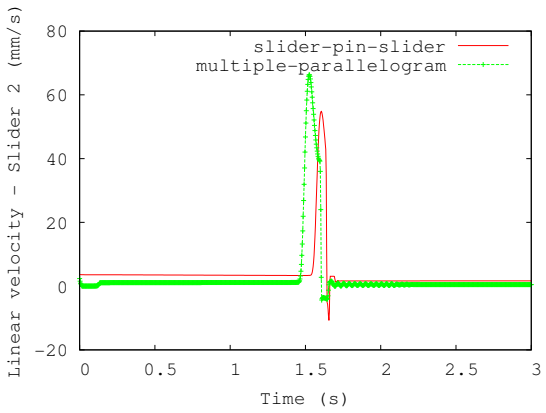

Figure 11. Simulation's result: linear velocity of the slider 2

hypothesis that we made in Section 3.3. On the other hand, we also notice that the torsional spring has a larger deflection in the case of the multiple-parallelogram mechanism which creates more important speeds at the self-adaption moment.

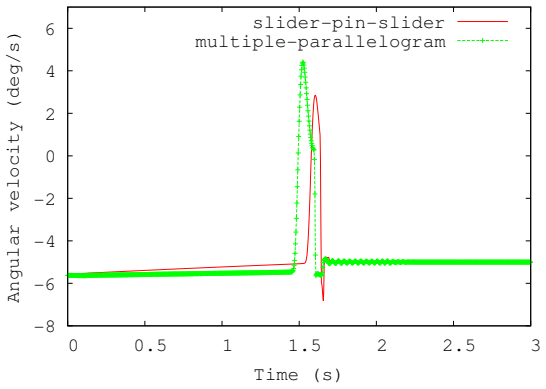

Figure 12. Simulation's result: the angular velocity of the hinge 1

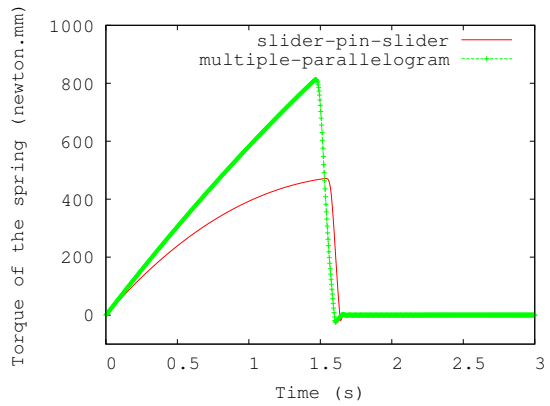

Figure 13. Simulation's result: the torque of the torsional spring

4.2 Simulation of the localization of the human joint'ICR

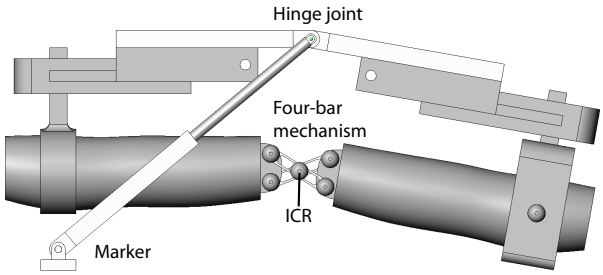

Figure 14. Mechanism used in the simulation to demonstrate the possibility of localizing the ICR of the limbs

In this simulation, a marker indicates the position of the ICR of the user's joint. The marker coincides initially with the hinge joint of the mechanism. We define two equations of movement for the extremity of the marker following the directions $\vec{x}$ and $\vec{y}$, according to the two expressions (5) and (6) obtained previously in the section 2.2.

In order to better cope with the real kinematics of the knee joint, we introduce a four bar mechanism with two intersecting slots defining the real location of the ICR of the knee joint. A torsional spring is added at the attachment of the mechanism on the 2nd limb.

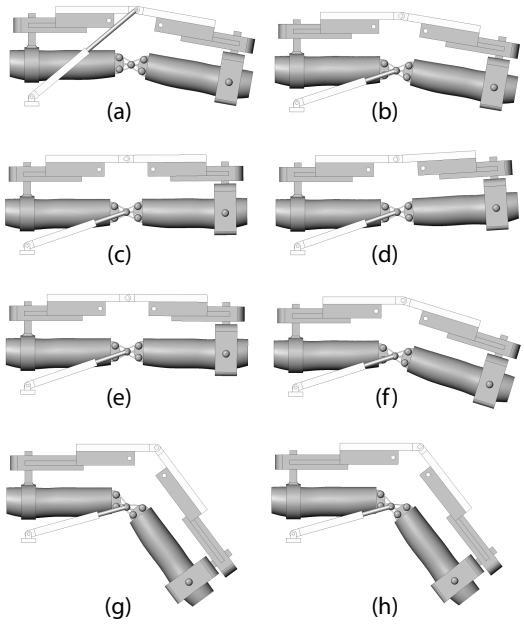

Figure 15. The evolution of the mechanisms during the simulation. a) The mechanism at its initial position. The marker is placed at the position of the hinge joint. (b) At the beginning of the motion, the marker moves so that its extremity coincides with the position of the ICR. (c) The mechanism crosses its singular position, a light oscillation takes place. (d) An abrupt change of rotational velocity takes place, the limb turns in the inverse direction, which generates an important oscillation. (e) The mechanism crosses its singular position again. (f) A new change of rotational velocity, but without changing the rotation direction, a short oscillation produces. (g) Another change of rotation speed in the opposite direction produces another short oscillation. (h) The marker pursues the trajectory of the ICR until the end of the simulation

The mechanism is initially placed in the position where the rotation angle of the hinge joint is -10 degree. A constant angular velocity (7 degree/s) is first set to the first hinge joint of the four-bar mechanism. At 1 second, the angular velocity is changed to -10 degree/s, then it will be changed to -20 degree/s at 2 second and to 5 degree/s at 2.8 second. A torsional spring (10 N.m/degree) is added to the attach-

ment's pin joint of the second limb. The two slider's friction coefficient is set at 0.001. The simulation ends at 3 second.

The figure 15 shows the evolution of the simulation. The results of the simulation confirm the results of the analysis made in section 2.2. Except the oscillations, the extremity of the marker indicates exactly the position of the ICR during its motion.

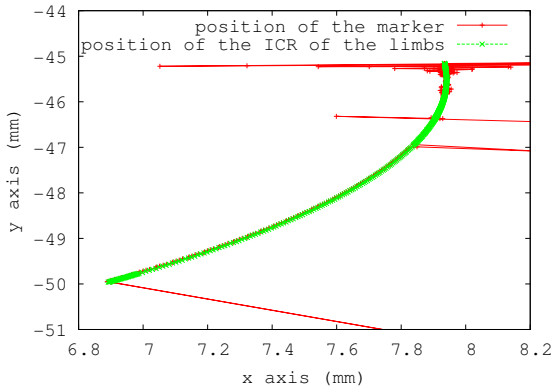

Figure 16. The trajectory of the ICR and the marker

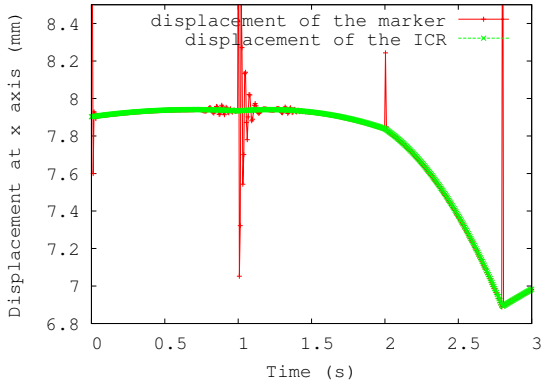

Figure 17. Displacement along the x-axis

As shown in the figures 16, 17 and 18, the results of the simulation verify the validity of the formula (5) and (6) established in Section 2.2. The extremity of the marker and the ICR are in coincidence during the motion. Light oscillations occur when the mechanism crosses its singular position (which happens at around 0.8 second and 1.2 second in this simulation). This is caused by the deflection of the torsional spring as the mechanism enters its singular configuration.

Oscillations may occur in case of abrupt changes of rotation speed of the user's joint. The duration of these oscillations is shorter than those caused by the moving of the mechanism through its singular position. However, we notice that if a non-smooth operation of the mechanism takes place at the same instant

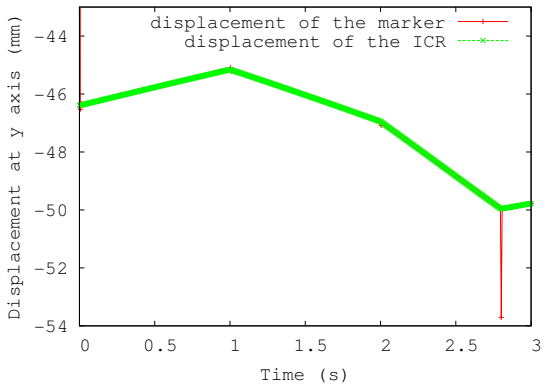

Figure 18. Displacement along the y-axis

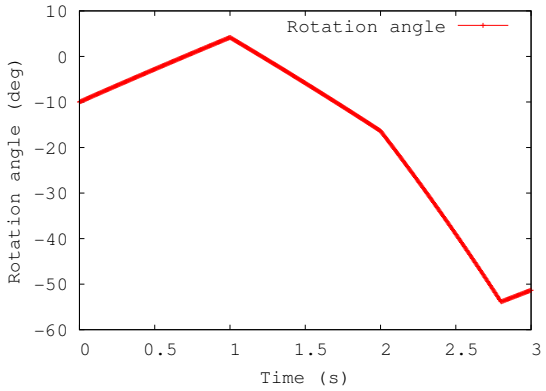

Figure 19. Rotation angle of the hinge joint

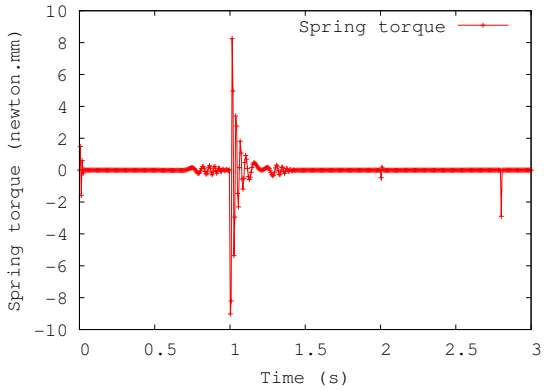

Figure 20. The spring torque

of the kinematic singularity crossing, an large oscillation may occur. We can observe this phenomenon at the moment of the first change of the angular velocity (when the simulation is at 1 second).

To reduce the amplitude of the oscillation, it is necessary to place the mechanism initially in its singular configuration and, at the same time, to increase

the stiffness of the torsional spring placed towards the attachment, which means that the attachments of the mechanism on the members must be tightened well. Abrupt movements must be avoided when the mechanism is near its singular position.

5 Conclusion

In this paper, we have demonstrated that it is possible to design orthosis devices which can self-adapt to a human joint's kinematics. As a by-product, these self-adjusting mechanisms can be used to estimate the effective axis of rotation during movement. These results show the possibility to build an intelligent orthosis which is able to track human joint and is adaptable to large human joints.

In future work, 3D mechanical designs will be studied in order to build orthoses which can track complex kinematics of human joints. Solutions for the self-adaption in both horizontal and vertical directions will also be examined. We will also take an interest in the control of these mechanisms.

Acknowledgements

The authors would like to thank Han Xu, trainee at ISIR - University Pierre et Marie Curie, for his contribution in the work of simulation, Guillaume Morel and Nathanaël Jarrasse for the discussions about the conception of active orthoses used in rehabilitation, Dr. Philippe Decq and his colleagues of the hospital Henri Mondor for their comments on this work.

References

[1] T. Herzberg, A. Albrod, Knee-Joint Orthosis, *United States Patent*, Pub. Num. 6,309,368 B1, Oct. 30, 2001.

[2] J. O'Connor, J. Goodfellow, The mechanics of the knee and prothesis design, *The Journal of Bone and Joint Surgery*, 1978.

[3] P.N. Smith, K.M. Refshauge and J.M. Scarvell, Development of the concepts of knee kinematics, *Archives of Physical Medicine and Rehabilitation*, 2003, Volume 84, Issue 12, 1895-1902.

[4] G. Lambert, Knee Orthosis, *United States Patent*, Pub. Num. US2006/0089581 A1, Apr. 27, 2006.

[5] S.R. Lamb, R. Moore, Anatomic Fracture Brace For The Knee, *United States Patent*, Pub. Num. 4,523,585, Jun. 18, 1985.

[6] G.V. Aaserude, R.H. Rubin, Polycentric Variable Axis Hinge, *United States Patent*, Pub. Num. 4,699,129, Oct. 13, 1987.

[7] V. Patel, K. Hall, M. Ries, J. Lotz, E. Ozhinsky, C. Lindsey, Y. Lu, S. Majumdar, A three-dimensional MRI analysis of knee kinematics, *Journal of Orthopaedic Research*, 2004, 283-292.

[8] K.L. Markolf, J.S. Mensch, and H.C. Amstutz, Stiffness and laxity of the knee–the contribution of the supporting structures. A quantitative in vitro study, *The Journal of Bone and Joint Surgery*, 1976, 58:583-594.

[9] K.L. Markolf, A. Graff-Radford, and H.C. Amstutz, In vivo knee stability. A quantitative assessment using an instrumented clinical testing apparatus, *The Journal of Bone and Joint Surgery*, 1978, 60:664-674.

[10] A. Gupta, M.K. O'Malley, V. Patoglu and C. Burgar, Design, Control and Performance of RiceWrist: A Force Feedback Wrist Exoskeleton for Rehabilitation and Training, *The International Journal of Robotics Research*, 2008.

[11] M. Casadio, P. Morasso, V. Sanguineti, P. Giannoni, Impedance-controlled, minimally-assistive robotic training of severely impaired hemiparetic patients, *Biomedical Robotics and Biomechatronics, 2006. BioRob 2006. The First IEEE/RAS-EMBS International Conference on* , 2006, 507-512.

[12] A. Forner-Cordero, J.L. Pons, E.A. Turowska and A. Schiele, Kinematics and dynamics of wearable robots, in José L. Pons (Ed.), *Wearable Robots - Biomechatronic Exoskeletons*, (Chichester, John Wiley and Sons, 2008) 70-74.

[13] A. Schiele and F.C.T. Van der Helm, Kinematic Design to Improve Ergonomics in Human Machine Interaction, *IEEE Transactions On Neural Systems And Rehabilitation Engineering*, 14(4), 2006.

[14] B.L. Shields, J.A. Main, S.W. Peterson, and A.M. Strauss, An Anthropomorphic Hand Exoskeleton to Prevent Astronaut Hand Fatigue During Extravehicular Activities, *IEEE Transactions On Systems, Man, And Cybernetic PART A: Systems And Humans*, 27(5), 1997.